Synthesis and characterization of nano-biomaterials with potential osteological applications

M. J. PHILLIPS, J. A. DARR, Z. B. LUKLINSKA, I. REHMAN
Interdisciplinary Research Centre in Biomedical Materials, Department of Materials, Queen Mary, University of London, Mile End Road, London, E1 4NS, UK
E-mail: i.u.rehmam@qmar.ac.uk

The manufacture of high-surface area, un-agglomerated nano-sized (1–100 nm) bioceramic particles are of interest for many applications including injectable/controlled setting bone cements, high strength porous/non-porous synthetic bone grafts, and the reinforcing phase in nano-composites that attempt to mimic the complex structure and superior mechanical properties of bone. In the present study, we report on the manufacture of nano-particle hydroxyapatite powders by several wet chemical methods, which incorporate a freeze-drying step.

In particular, it was found that the emulsion-based syntheses yielded powders with high surface areas and small primary particle sizes. Freeze drying rather than oven drying of powders prepared by conventional wet chemical synthesis yielded a nano-sized powder with a comparatively higher surface area of 113 m^2/g. All powders were calcined in air in a furnace at 900 °C to investigate the effects of synthesis method on phase purity and surface area. The materials were characterized by a range of analytical methods including Fourier-transform infrared spectroscopy employing the photo acoustic (PAS-FTIR) sampling technique, BET surface area analysis, X-ray powder diffraction (XRD), and the particles were examined using a transmission electron microscope (TEM).
© *2003 Kluwer Academic Publishers*

1. Introduction

Cortical bone is made up of a nano-particle crystalline calcium phosphate phase and an organic phase largely made up of type I collagen fibers. The mineral calcium phosphate phase in bone can be characterized as a nonstoichiometric substituted apatite [1]. Hydroxyapatite $[Ca_{10}(PO_4)_6(OH)_2]$ is a synthetic calcium phosphate material that has similarities to the mineral component of human bone. Hydroxyapatite is classed as a bioactive ceramic that is available commercially for use in bone replacement applications. Hydroxyapatite can be manufactured synthetically by using a number of different methods.

In general, conventional wet chemical syntheses of ceramic powders (also referred to as ''bulk'' precipitation) can often yield powders with large primary particles, wide particle size distributions and relatively low surface areas (less than 100 $m^2\,g^{-1}$ for as prepared materials). This is due to the inability to effectively control flocculation of particles as they are formed. Thus, quite often a ball-milling step is required in order to produce fine less agglomerated particles.

''Water in oil'' emulsion methods have been known for some time as convenient vesicles for the synthesis of fine ceramic powders of electronic, magnetic and optical materials [2]. However, in comparison, there are very few reports of the use of such emulsions for the synthesis of nanoparticle calcium phosphates [3, 4]. ''Water in oil'' emulsions act as small nano- or micron-sized water containing reactors, which effectively reduce particle flocculation and to some extent limit particle growth. The increase in interfacial area of the water provided by an emulsion and the controlled size, and potentially uniform shape of the water ''droplets'' can be very useful in the processing and manufacture of small particulate materials [5]. Thus, precipitation reactions carried out in the cores of such systems should yield smaller particles that form powders with higher surface areas compared to ''bulk'' aqueous precipitation reactions.

In the majority of reported synthesis for bioceramic powders, there is usually very little attention given to the drying step of the freshly precipitated material. Prolonged oven drying (e.g. for 24 h/110 °C) is by far the most favored method for removal of water from the

precipitated filter cake [6]. Such a step is undoubtedly convenient, but will no doubt significantly affect the physical properties of the precipitate.

In this paper, we report on the production of high-surface area hydroxyapatite powders by emulsion or conventional ''bulk'' syntheses, respectively followed by freeze-drying (instead of oven drying). The effects of high temperature calcination upon powder properties are also reported.

2. Materials and methods

2.1. Chemicals

Deionized water (10 M Ω) from an USF Elga Option 2 Deionizer was used in all reactions. The sodium salt of dioctylsulfosuccinate (AOT) and isooctane were used as purchased (Aldrich Chemicals, Dorset, UK) for the oil phase of the emulsion. Calcium hydroxide, $Ca(OH)_2$ (analytical grade), and 85% assay orthophosphoric acid (GPR grade), H_3PO_4, were used as supplied (Merck Eurolab, UK). The ammonia solution used as supplied (Merck Eurolab, UK), NH_3OH Anal R.

2.2. Syntheses of powders

2.2.1. Method A: ''bulk'' precipitation

Wet chemical synthesis was carried out using orthophosphoric acid [H_3PO_4] solution (34.59 g in 1000 ml to give a 0.3 M aqueous solution) which was added dropwise to a suspension of calcium hydroxide [$Ca(OH)_2$] (37.31 g in 1000 ml of water to give a 0.503 M conc). This gives a Ca : P ratio of 1.667 for the reagents. The pH of the suspension was adjusted to 10.5 by the dropwise addition of concentrated ammonia solution followed by stirring for 4 h. After stirring, the suspension was further kept for 18 h to allow completion of the reaction. The mixture was then filtered and washed with 2 × 100 ml aliquots of cold water and the wet filter cake was freeze-dried for 18 h to obtain a fine white powder (35 g; yield = 69%).

2.2.2. Method B: macroemulsion reaction

1000 ml of a 0.1 M solution of AOT in isooctane (44.45 g in 1000 ml) was made-up and stirred for 30 min. To this mixture, an aqueous suspension of $Ca(OH)_2$ (7.46 g in 200 ml of H_2O, 0.103 mol) was added dropwise and allowed to stir for 15 min. It was followed by dropwise addition of an aqueous solution of H_3PO_4 (6.92 g in 200 ml of H_2O, 0.06 mol) to the AOT/isooctane/$Ca(OH)_2$ emulsion. The pH of the emulsion was adjusted to 10.5 by the drop wise addition of concentrated ammonia solution. The total volume of water used in the reaction equated to 40% water in oil (macroemulsion) and the ratio of Ca : P was 1.677. The emulsion was stirred for 24 h and the mixture filtered followed by washing with 2 × 100 ml aliquots of cold water. The wet filter cake was freeze-dried for 18 hrs to give a fine white powder (5.3 g; yield = 52%).

2.2.3. Method C: microemulsion reaction

A similar reaction procedure as described for method B was used. However, the total water in oil volume was 10% (microemulsion). 1000 ml of a 0.1 M solution of AOT in isooctane (44.45 g in 1000 ml) was made-up and stirred for 30 min. To this mixture, 50 ml of the aqueous suspension $Ca(OH)_2$ (3.73 g in 100 ml of H_2O, 0.0503 mol) was added dropwise and allowed to stir for 15 min. Then 50 ml of the aqueous solution of H_3PO_4 (3.46 g in 100 ml of H_2O, 0.03 mol) was added dropwise to the AOT/isooctane/$Ca(OH)_2$ emulsion. The pH of the emulsion was adjusted to 10.5 by the drop wise addition of concentrated ammonia solution. However, the pH fell slightly lower than 10.5 near the end of the reaction. The emulsion was stirred for 24 h followed by filtration and then washed with 2 × 100 ml aliquots of cold water. The wet filter cake was freeze-dried for 18 h to give a fine white powder (2.4 g; yield = 47%).

2.3. Equipment

2.3.1. Freeze-drying

All powders produced in this study were freeze-dried using an Edwards 4K Modulyo Freeze Dryer; wet filter cakes were rapidly frozen using liquid nitrogen and then dried at ca. 10^{-1} mbar for ca. 18 h.

2.3.2. Calcination of powders

A proportion of each powder was calcined in a Carbalite tube furnace in air using the following heating rate; heated from room temperature at 2.5 °C/min up to 900 °C, held at this temperature for 2 h and then cooled down to room temperature at 10 °C/min.

2.3.3. Fourier transform infrared spectroscopy

FTIR spectra for the powders were obtained using a Nicolet 800™ FTIR spectrometer in conjunction with an Mtech™ Photo Acoustic Sampling (PAS) cell. Spectra were obtained at 4 cm^{-1} resolution, averaging 128 number of scans. The sample chamber of the PAS cell was purged with dry helium gas (pre-dried over a column of magnesium perchlorate).

2.3.4. X-ray powder diffraction

X-ray powder diffraction (XRD) patterns were collected for the powder samples using a Siemens D5000 diffractometer using Cu–K_α radiation ($\lambda = 0.15418$ nm). Data was collected over the 2θ range 25–40° with a step size of 0.2° and step time of 2.5 s. Identification of phases was achieved by comparing the diffraction pattern obtained to the Joint Committee on Powder Diffraction Standards (JCPDS) database.

2.3.5. BET surface area analysis

The specific surface area of the powders was determined by the Brunauer–Emmett–Teller (BET) method using a Micromeritics Gemini II 2370 surface area analyzer. The powdered samples were degassed using a Flow Prep 060 controller at 200 °C for 3 h prior to analyses.

2.3.6. Transmission electron microscopy

The particles were studied in a JEOL JEM 2010 high resolution transmission electron microscope (TEM) operated at 200 KeV. Samples were prepared by ultrasonically dispersing the powders in methanol prior to collection on carbon coated copper grids. Morphology and average particle size were estimated from the bright field images. Selected area diffraction patterns (SADP) were also taken in order to confirm the nature and composition of the powders.

3. Results and discussion

3.1. Synthesis and terminology

The ''bulk'' wet chemical synthesis of hydroxyapatite method (used as a ''control'' reaction in this study) was modified from an identical method reported elsewhere [7]. In the study reported here, the powder was filtered to a soft wet filter cake and then freeze-dried for 18 h. This resulted in a material that could easily be broken up into a free flowing powder. In comparison, powders dried using oven drying were more ''compact'' and possess a significantly lower surface area.

In a recent report, Lim *et al*. [8] have investigated the use of biodegradable surfactants such as alcohol ethoxylate for the manufacture of hydroxyapatite. The surfactant used herein was the sodium salt of 1,4-bis(2-ethylhexyl sulfosuccinate (AOT) and the oil phase used was isooctane. This surfactant is the most widely employed for inverse emulsions because it readily forms well-characterized reverse micelles (organic ''tails'' point out into the oil whilst charged ''head'' groups point into water ''droplet'') over a wide range of water/surfactant mole ratios (see Fig. 1).

Essentially, a microemulsion is an emulsion where the volume of water in the oil is small enough so that the emulsion remains transparent and is stable indefinitely for a long but defined time (in this study for a water vol less than 11%; we used 10%). In comparison, a macroemulsion is formed when the volume of water is large enough to cause the emulsion to become opaque and only remains stable by continued stirring (we used 40%; powder B).

It has been reported in the literature that HA can form needle-shaped crystallites that have preferential growth in the [0 0 2] direction [9]. In our studies, the as prepared powders for all reactions also produce needle-like particles, hence the emulsions may not be affecting the particle shape. However, the particles made from emulsions (B and C) are smaller in size than those from the ''bulk'' precipitation route (method A) prior to calcination. Thus, the emulsions appear to be limiting particle growth. TEM analyses of powder produced by method C revealed particles of ca. 100 × 5 nm (Fig. 2). In comparison, the primary particle size of powders produced by method A were ca. 150 × 20 nm (Fig. 3). Both types of powder have very well defined, needle-shaped particles. These fine crystallites gave rise to strong and slightly diffused full rings in the SADP (see inserts in Figs. 2 and 3). After calcination, powders from emulsion methods B and C respectively, formed larger crystallites of 220 × 115 nm, compared to those from method A (75 × 50 nm), presumably due to the superior wettability of the latter (Figs. 4 and 5, respectively). The

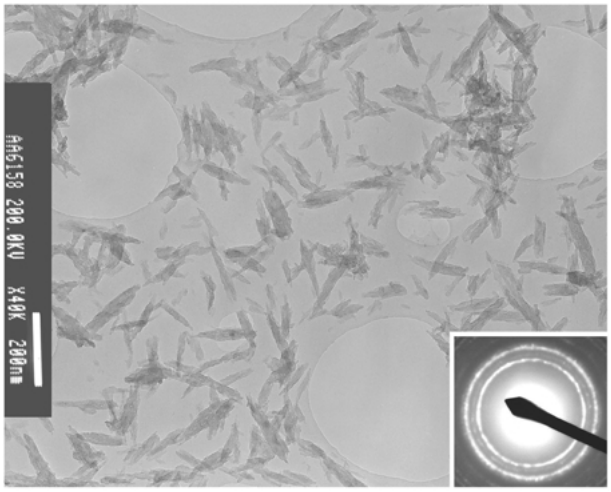

Figure 2 TEM and SADP of powder C hydroxyapatite particles after freeze-drying for 18 h.

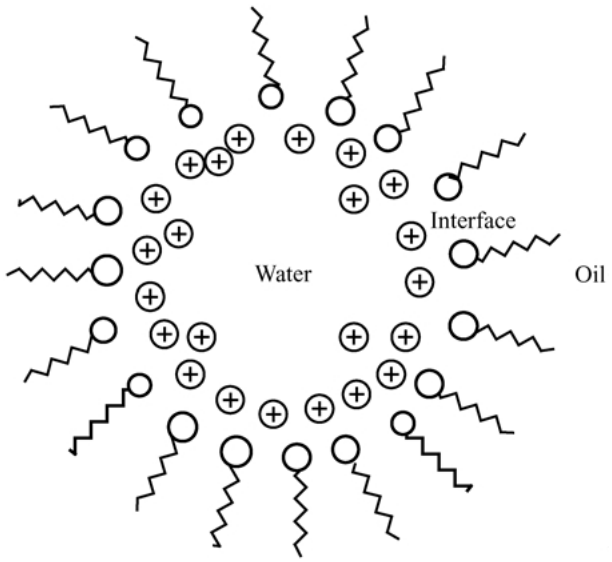

Figure 1 Representation of AOT reverse micelles.

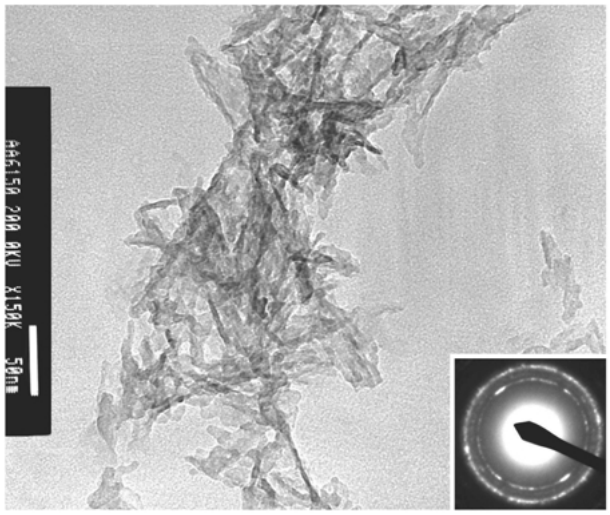

Figure 3 TEM and SADP showing needles of hydroxyapatite powder A after freeze-drying for 18 h.

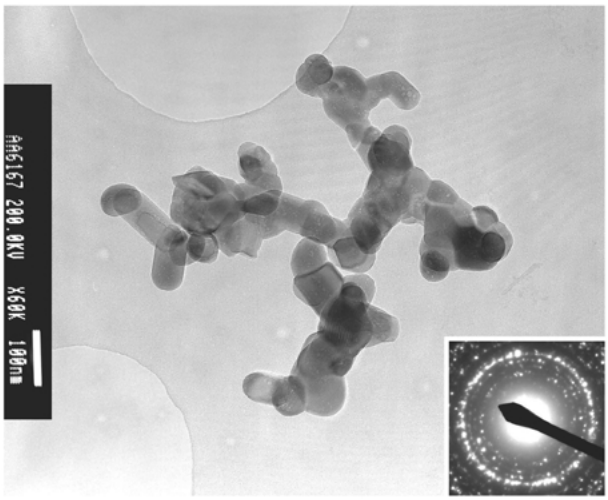

Figure 4 TEM and SADP showing needles of hydroxyapatite powder A after freeze-drying for 18 h and then calcination in air at 900 °C for 2 h.

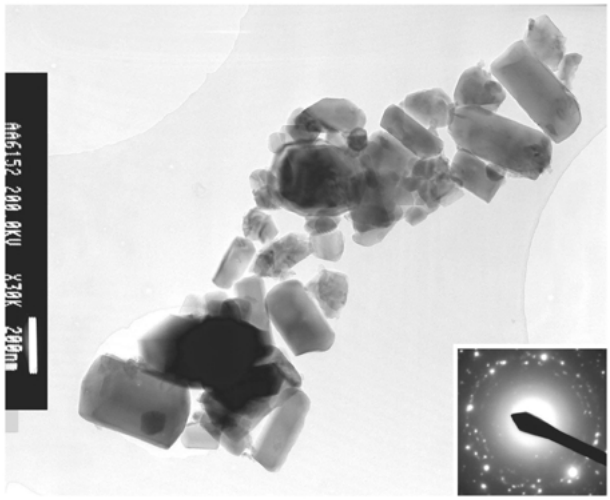

Figure 5 TEM and SADP of powder C hydroxyapatite particles after freeze-drying and then calcination in air at 900 °C for 2 h.

reduced number of larger crystallites resulted more spot-like SAD patterns as seen in Figs. 4 and 5.

The surface area of the powders was measured using Brunauer–Emmett–Teller (BET) surface area analysis and the results before and after calcinations are summarized in Fig. 9. Freeze-drying of hydroxyapatite prepared using the ''bulk'' wet chemical method produced a powder (A) with a surface area of 113 m^2/g. In comparison, similar methods for producing HA in the literature using oven drying (for up to 24 h/ca. 100 °C), give powders with lower surface areas in the range 55–90 m^2/g [10]. This suggests that oven drying of as prepared HA powders results in ''aging'' or agglomeration, which significantly lowers the surface area of the material. Freeze drying has the effect of drying small sections of precipitate at a time with much less opportunity for particles to agglomerate. The as-precipitated powders made using macro and microemulsions had very similar surface areas (215 & 218 m^2/g for B and C, respectively). Notably, the surface areas of the powders prepared in emulsions are almost three times that prepared using traditional ''bulk'' precipitation/oven drying methods.

Calcination in air had the effect of reducing the surface area of powder A to 19 m^2/g, which is comparable to that for hydroxyapatite prepared using oven drying in the literature (15 m^2/g) [11]. The reduction in surface area of hydroxyapatite powders B and C upon calcination was more significant. Both powders were reduced to a surface area of ca. 1 m^2/g, suggesting that the as prepared, emulsion synthesized powders had a much greater wetability compared to powder A. This is due to a

TABLE I Measured *d* lattice plane spacing compared to HA JCPDS database card values

Measured *d* (nm)	0.350	0.315	0.285	0.232	0.200	0.189	0.175	0.148
HA *d* (JCPDS card)	0.351	0.317	0.281	0.230	0.200	0.189	0.175	0.147

TABLE II FTIR peak assignments for the as prepared hydroxyapatite powders after freeze-drying

Peak assignments cm^{-1}	Merck HA	Freeze-dried	Macroemulsion	Microemulsion
Hydroxyl stretch	3570	3569 (w, br)	3570 (w, br)	3570 (w, br)
Carbonate v_3				
(m)	1648	1650 (w, br)	1620 (st, br)	1733 (st, br)
(m)	1455	1450 (w, br)	1470 (st, br)	1463 (st, br)
(m)	1417	1410 (w, br)	1420 (st, br)	1416 (st, br)
(w)	/	/	/	1248 (st, br)
Phosphate v_3				
(vs)	1091	/	/	/
(vs)	1042	1028 (st, br)	1030 (st, br)	1029 (st, br)
Phosphate v_1				
(m)	962	960 (w)	962 (w)	962 (w)
Carbonate v_2				
(ms)	877	890 (w)	876 (w, sh)	894 (w)
Phosphate v_4				
(m)	632	/	/	/
(vs)	602	605 (st, br)	602 (w, sh)	604 (w, br)
(vs)	566	563 (st, br)	581 (w, sh)	562 (w, br)
Phosphate v_2				
(w)	472	490 (w)	478 (w)	470 (w)

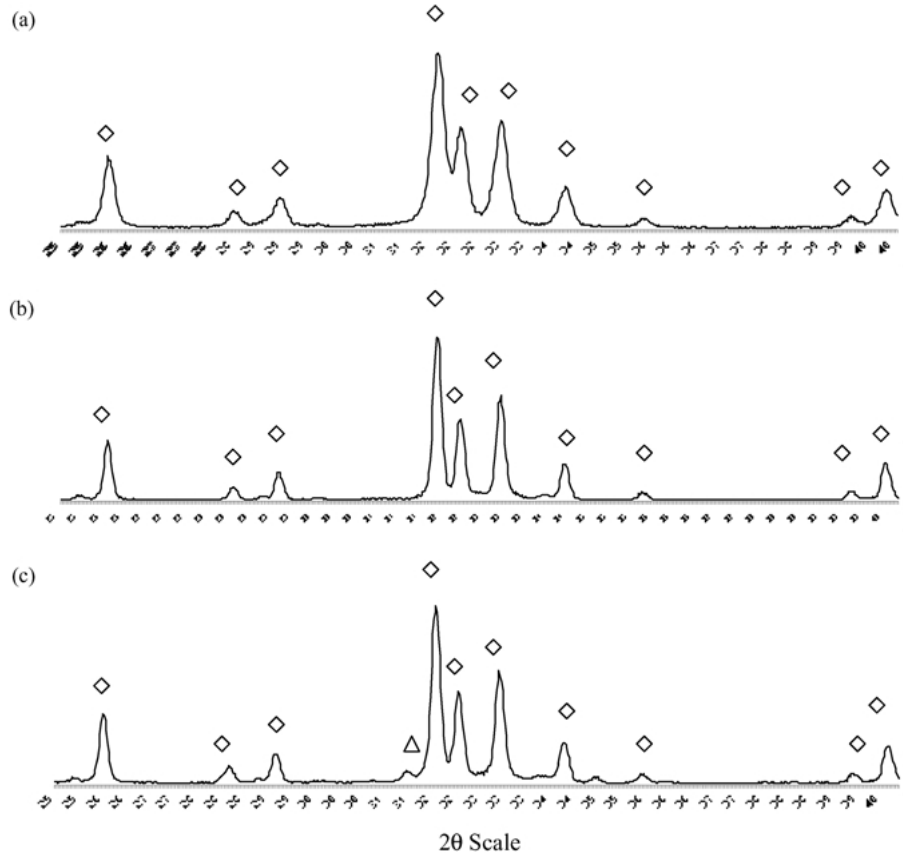

Figure 6 XRD traces for powders A, B and C after calcined in air at 900 °C for 2 h [09-0432 (I) – Hydroxylapatite, syn – $Ca_5(PO_4)_3(OH)$ and △ 09-0169 (I) – Whitlockite, syn – $Ca_3(PO_4)_2$].

''fusing'' of the small particles of the high surface area ''emulson'' powders in order to lower the total surface free energy by the reduction of solid-vapor interface [12]. These results have important implications for the manufacture of dense/defect free bioceramic implants.

In all cases, the nano-size of ''as precipitated'' powders and the crystallites formed after freeze-drying led to very broad peaks being observed in the XRD traces. Hence, it was difficult to estimate the exact phase composition of the calcium phosphates from these traces. After calcination in air at 900 °C for 2 h, the XRD traces were more revealing due to the increased crystallite size. Phase pure hydroxyapatite [JCPDS pattern 09-0432] was almost exclusively present in all cases (see Fig. 6). Only the XRD trace for the calcined ''microemulsion'' hydroxyapatite (Powder C) revealed a minor impurity, which was identified as tricalcium phosphate (Whitlockite, $Ca_3(PO_4)_2$); JCPDS database card 09-0169 (Fig. 6). The tricalcium phosphate (TCP) impurity is believed to have formed due to the drop in pH near the end of the emulsion reaction. This indicates that there is an opportunity to produce other calcium phosphate phases, such as pure TCP, within an emulsion by maintaining a lower pH. The XRD peaks for the calcined powders from the two emulsion reactions were noticeably sharper than the peaks for the corresponding (calcined) ''bulk'' precipitated powder A, suggesting larger particles for the former. Measurements taken from the SADP confirmed that all samples, as prepared and calcined, were composed of crystalline HA. There was no evidence in these readings of any other compounds, such as tricalcium phosphate (TCP). Table I shows measurements taken for as prepared powder A (Fig. 2). The values for the *d* lattice plane spacing match well with data for HA from the JCPDS database card 09-0169. Similar measurements taken from other SAD patterns (Figs. 3–5) are consistent with the values found for powder A and confirm the presence of HA.

The FTIR spectra for the as prepared and calcined hydroxyapatite, respectively are similar and the peaks correlate well with studies reported previously by Rehman *et al*. [13]. See Tables II and III for peak assignments for as-prepared and calcined powders respectively. Additional peaks are also observed for the calcined emulsion-produced hydroxyapatite powders at around 2000 and 2077 cm^{-1}. These peaks were thought to be due to bicarbonate (HCO_3^-) but could be the ν_3 cyananmide and/or cyanate band [14, 15]. This may be because of the increased amount of ammonia added during the hydroxyapatite synthesis. Ammonia is added during synthesis of hydroxyapatite to increase the pH of the reaction mixture and encourage the formation of hydroxyapatite. In this emulsion, the pH is initially much lower and more ammonia is required to raise the mixture to the required pH of 10.5. In some instances the as precipitated emulsion-manufactured batches of hydroxyapatite have included peaks that do not initially appear to be related to the Na-AOT surfactant. Such peaks appear between 2870 and 2970 cm^{-1} and are believed to be from C–C bonds, which are most likely to be a residual from the AOT surfactant.

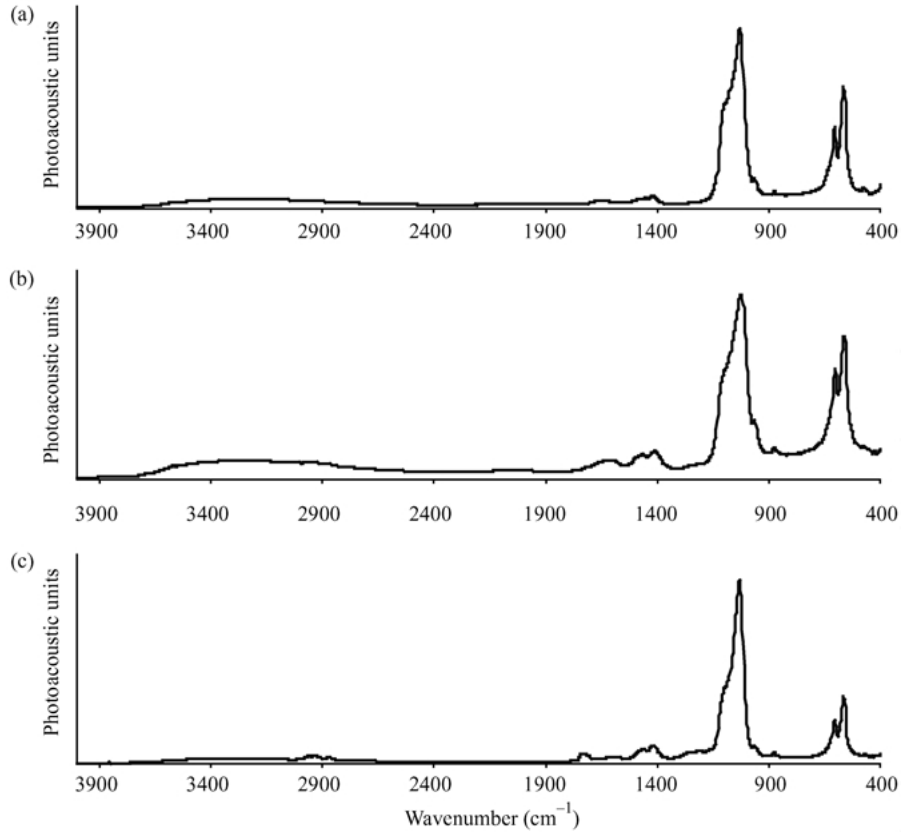

Figure 7 FTIR spectra for the as prepared powders A, B and C after freeze-drying for 18 h.

Weak hydroxyl (O–H) stretches were observed in the FTIR spectra for all powders at ca. 3570 cm^{-1} (see Figs. 7 and 8). In contrast, the hydroxyl peaks for the calcined powders were considerably sharper. The intensity of the hydroxyl peak is commonly reduced after calcination but in this case it has become more defined. The reduced intensity of the hydroxyl peaks for the fresh powders could be due to a residual coating of the surfactant phase on the hydroxyapatite particles after washing and filtering. However, the freeze-dried powder showed the

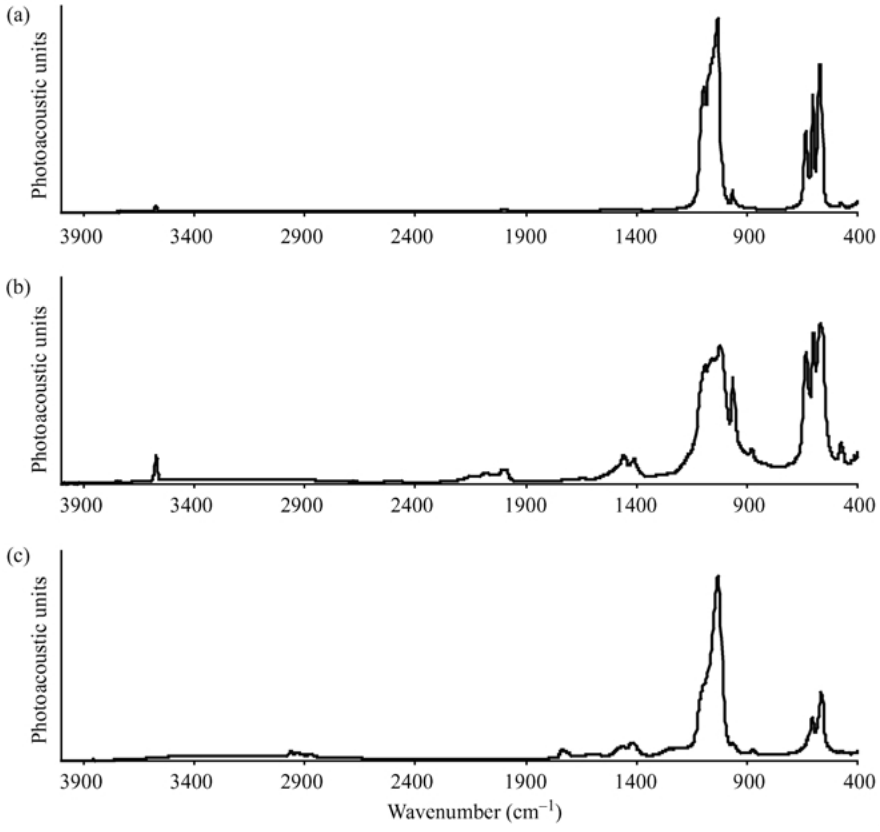

Figure 8 FTIR spectra for powders A, B and C after freeze-drying for 18 h and calcined at 900 °C for 2 h.

TABLE III FTIR peak assignments for the hydroxyapatite powders after freeze-drying and calcining at 900 °C for 2 h

Peak assignments cm^{-1}	Merck HA	Freeze-dried	Macroemulsion	Microemulsion
Hydroxyl stretch	3570	3571 (w, sh)	3571 (st, sh)	3570 (st, sh)
Carbonate v_3				
(m)	1648	/	/	/
(m)	1455	/	1450 (w, sh)	/
(m)	1417	/	1410 (w, sh)	/
(w)	/	/	/	/
Phosphate v_3				
(vs)	1091	1093 (st, sh)	1087 (st, sh)	1088 (st, br)
(vs)	1042	1031 (st, sh)	1019 (st, sh)	1022 (st, br)
Phosphate v_1				
(m)	962	963 (st, sh)	962 (st, sh)	962 (st, sh)
Carbonate v_2				
(ms)	877	891 (w)	878 (w, sh)	892 (w)
Phosphate v_4				
(m)	632	633 (st, sh)	630 (st, sh)	631 (st, sh)
(vs)	602	602 (st, sh)	539 (st, sh)	600 (st, sh)
(vs)	566	568 (st, sh)	560 (st, sh)	567 (st, sh)
Phosphate v_2				
(w)	472	474 (sh)	474 (w, sh)	490 (w, sh)

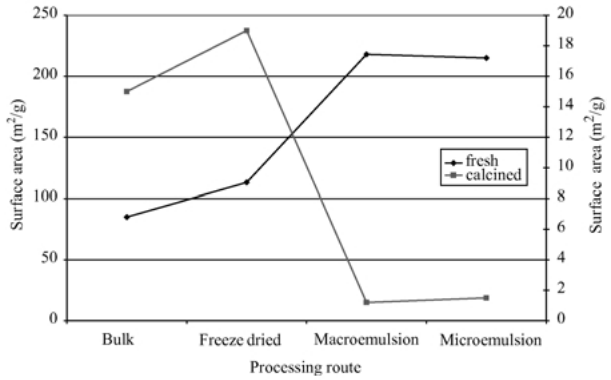

Figure 9 Plot to show the variation in specific surface area (BET analysis) with different processing routes.

same weak hydroxyl peak in its fresh form. These findings indicate that the definition of the hydroxyl peak is increased, as the surface area reduces and particle size increases. It is possible that although calcination causes a reduction in surface area, the remaining surface hydroxyl groups are in positions that are more easily observed by FTIR.

The carbonate v_3 peaks are observed in the region of 1240 and 1740 cm^{-1} for the fresh powders and they appear at 1650, 1450 and 1410 cm^{-1} for the wet chemical, freeze-dried powder. The calcined powders have very weak carbonate bands although the macroemulsion hydroxyapatite has stronger bands at 1450 and 1410 cm^{-1} due to carbonate (ν_3) symmetric stretch. All powders, fresh and calcined, have the carbonate v_2 bands in the region 875 to 895 cm^{-1}. The ν_2 band is sharper in the calcined powders.

In each of the as prepared powders, a single band due to phosphate stretching vibration (ν_3) is seen in the range 1028–1030 cm^{-1}. The calcined powders have phosphate v_3 sites at 1010 or 1030 and around 1090 cm^{-1}. The phosphate (ν_1) stretch is present at around 960 cm^{-1} in all spectra of the powders and is sharper in the calcined powders. Two phosphate (ν_4) bands at 600 and 560 cm^{-1}, respectively, are observed in the FTIR spectra of the as prepared materials. In comparison, the FTIR spectra for the calcined powders revealed an additional peak at 630 cm^{-1}. The phosphate ν_2 band is observed in the range of 470–490 cm^{-1}. These are very weak bands, which are slightly stronger in the calcined powders.

4. Conclusion

The results obtained in this study revealed that a significant retention of surface area could be achieved by freeze-drying of the wet hydroxyapatite filter cakes after (''bulk'') co-precipitation compared to the conventional oven drying method. Undoubtedly, the use of oven drying of wet filter cakes results in significant agglomeration of particles and loss in total surface area (as much as 30%).

Free flowing powders containing nano-sized particles of hydroxyapatite with relatively large surface areas ($> 200\ m^2\ g^{-1}$) can be synthesized in the cores of water in oil emulsions that contain as much as 40% water content. The synthesized HA powder properties were not significantly different between emulsions containing either 10 or 40% volumes of water in oil phase. Particles prepared by such a route showed excellent wettability when calcined and as a result would be expected to show superior sinterability for the formation of dense, defect-free sintered ceramic discs, providing increased mechanical properties. These ceramics would be suitable for orthopedic applications such as bone plates, acetebular cups and coatings. Future studies to ascertain the effects of powder properties with respect to sintering and the subsequent mechanical properties are required and are in progress and will be reported in due course.

Acknowledgments

Continuous financial support of the EPSRC for the IRC core grant is gratefully acknowledged and especially the support of the EPSRC Advanced Research Fellowship of Dr Darr (JAD). We would also like to thank Dr I. Gibson for helpful discussions and Mr D. Porter for the technical support.

References

1. I. REHMAN, R. SMITH, L. L. HENCH and W. J. BONFIELD, *J. Biomed. Mater. Res.* **29** (1995) 1287.
2. G. H. MAHER, C. E. HUTCHINS and S. D. ROSS, *J. Mater. Proc. Tech.* **56** (1996) 200.
3. T. FURUZONO, D. WALSH, K. SCOTO, K SONODA and J. TANAKA, *J. Mater. Sci. Let.* **20** (2001) 111.
4. G. K. LIM, J. WANG, S. C. NG and L. M. GAN, *Mater. Let.* **28** (1996) 431.
5. D. SEGAL, *J. Mater. Chem.* **7** (1997) 1297.
6. S. ZHANG and K. E. GONSALVES, *J. Mater. Sci.: Mater. Med.* **8** (1997) 25.
7. A. OSAKA, Y. MUIRA, K. TAKEUCHI, M. ASADA and K. TAKAHASHI, *ibid.* **2** (1991) 51.
8. G. K. LIM, J. WANG, S. C. NG and L. M. GAN, *J. Mater. Chem.* **9** (1999) 1635.
9. R. KUMAR, P. CHEANG and K. A. KHOR, *J. Mater. Proc. Tech.* **113** (2001) 456.
10. P. SHUK, W. L. SUCHANEK, T. HAO, E. GULLIVER, R. E. RIMAN, M. SENNA, K. S. TENHUISEN and V. F. JANAS, *J. Mater. Res.* **16** (2001) 1231.
11. N. PATEL, I. R. GIBSON, S. KE, K. E. BEST and W. BONFIELD, *J. Mater. Sci.: Mater. Med.* **12** (2001) 181.
12. W. D. KINGERY, in ''Introduction to Ceramics'' (John Wiley & Sons, 1990) p. 469.
13. I. REHMAN and W. BONFIELD, *J. Mater. Sci.: Mater. Med.* **8** (1997) 1.
14. S. E. P. DOWKER and J. C. ELLIOT, *J. Solid. State. Chem.* **49** (1983) 334.
15. S. E. P. DOWKER and J. C. ELLIOT, *Calcif. Tiss. Int.* **29** (1979) 177.

Received 7 August 2002
and accepted 17 April 2003